JACS
JOURNAL OF THE AMERICAN CHEMICAL SOCIETY
Cite This: J. Am. Chem. Soc. 2019, 141, 14565−14569
Communication
pubs.acs.org/JACS

Self-Assembled Fluorescent Pt(II) Metallacycles as Artificial Light-Harvesting Systems

Koushik Acharyya,*[,†] Soumalya Bhattacharyya,[‡] Hajar Sepehrpour,[†] Shubhadip Chakraborty,[¶] Shuai Lu,[§,∥] Bingbing Shi,[†] Xiaopeng Li,[§] Partha Sarathi Mukherjee,*[,‡] and Peter J. Stang*[,†]

[†]Department of Chemistry, University of Utah, 315 South 1400 East, Room 2020, Salt Lake City, Utah 84112, United States
[‡]Department of Inorganic and Physical Chemistry, Indian Institute of Science, Bangalore 560012, India
[¶]Institut de Physique de Rennes, UMR CNRS 6251, Université de Rennes 1, Campus de Beaulieu, 35042 Rennes Cedex, France
[§]Department of Chemistry, University of South Florida, 4202 East Fowler Avenue, Tampa, Florida 33620, United States
[∥]College of Chemistry and Molecular Engineering, Zhengzhou University, Zhengzhou, Henan 450001, China

Supporting Information

ABSTRACT: Light-harvesting is one of the key steps in photosynthesis, but developing artificial light-harvesting systems (LHSs) with high energy transfer efficiencies has been a challenging task. Here we report fluorescent hexagonal Pt(II) metallacycles as a new platform to fabricate artificial LHSs. The metallacycles (**4** and **5**) are easily accessible by coordination-driven self-assembly of a triphenylamine-based ditopic ligand **1** with di-platinum acceptors **2** and **3**, respectively. They possess good fluorescence properties both in solution and in the solid state. Notably, the metallacycles show aggregation-induced emission enhancement (AIEE) characteristics in a DMSO−H_2O solvent system. In the presence of the fluorescent dye Eosin Y (ESY), the emission intensities of the metallacycles decrease but the emission intensity of ESY increases. The absorption spectrum of ESY and the emission spectra of the metallacycles show a considerable overlap, suggesting the possibility of energy transfer from the metallacycles to ESY, with an energy transfer efficiency as high as 65% in the **4**[a]**+ESY** system.

Photosynthesis is the main energy source for the survival of the living world. The natural photosynthesis process that takes place in green plants and other organisms starts with the absorption of light energy (sunlight) by a large number of closely packed green pigments (chlorophyll) embedded in a complex known as an antenna protein or a light-harvesting complex.[1] Subsequently, the absorbed energy funnels through chlorophylls to the reaction center, where light energy transforms into chemical energy (carbohydrates, like sugar). Inspired by nature, chemists have developed several artificial light-harvesting systems (LHSs) to understand the key aspects of the process and the intricacies of the mechanism along with their potential applications in photosynthesis, photocatalysis, and photovoltaics. In this context, wide varieties of scaffolds such as dendrimers,[2] organo- or hydrogels,[3] vesicles,[4] micelles,[5] host−guest assemblies,[6] metal−organic frameworks,[7] organic polymers,[8] and so on have been utilized in the past few years.

There are two prime factors that should be taken into account to achieve high energy collection efficiency in LHSs: (I) the system should possess multiple donors per acceptor, and (II) the donors should not suffer fluorescence quenching in their closely packed arrangements.

The LHSs reported to date could be broadly classified into two categories: (a) covalently bonded networks and (b) self-assembled architectures. The former group has the advantage of providing a stable platform, but it requires laborious synthetic steps. In contrast, self-assembled architectures could be easily obtained by mixing appropriate building blocks under suitable conditions. Therefore, supramolecular coordination complexes (SCCs) with easy synthetic accessibility, well-defined shapes, sizes, easy solution processability, and tunable photophysical properties could be interesting materials for light harvesting.

Over the past few decades, several SCCs, like one-dimensional (1D) helices, two-dimensional (2D) polygons, and three-dimensional (3D) polyhedrons, have been developed utilizing the directional coordination bonding approach.[9] Such SSCs are found to be attractive materials owing to their widespread applications in catalysis,[10] sensing,[11] biomedical science,[12] proton conduction,[13] and so on. Although several luminescent platinum-based metallacycles and cages have been reported,[14] their application toward light harvesting is in its infancy.[15] We report here two new fluorescent hexagonal platinum(II) metallacycles, **4** and **5** (Figure 1), along with their light-harvesting properties.

The desired metallacycles were designed and synthesized from ditopic organic donor **1** and di-platinum(II) acceptors **2** and **3** (Figure 1). Ligand **1** has a triphenylamine core with a cyanostilbene moiety decorated with an alkyl chain bearing a phenyl group, which could facilitate supramolecular assembly formation through non-covalent interactions.[16] The cyanostilbene moiety has interesting optical properties of aggregation-induced emission enhancement (AIEE), as a result of their restricted rotation in the aggregate state.[17] Moreover, the cyanostilbene moieties promote self-assembly to form various nano-architectures. Accordingly, the metallacycles may easily

Received: August 4, 2019
Published: September 3, 2019

Downloaded via INDIAN INST OF SCIENCE on October 12, 2022 at 09:50:57 (UTC).
See https://pubs.acs.org/sharingguidelines for options on how to legitimately share published articles.

© 2019 American Chemical Society

DOI: 10.1021/jacs.9b08403
J. Am. Chem. Soc. 2019, 141, 14565−14569

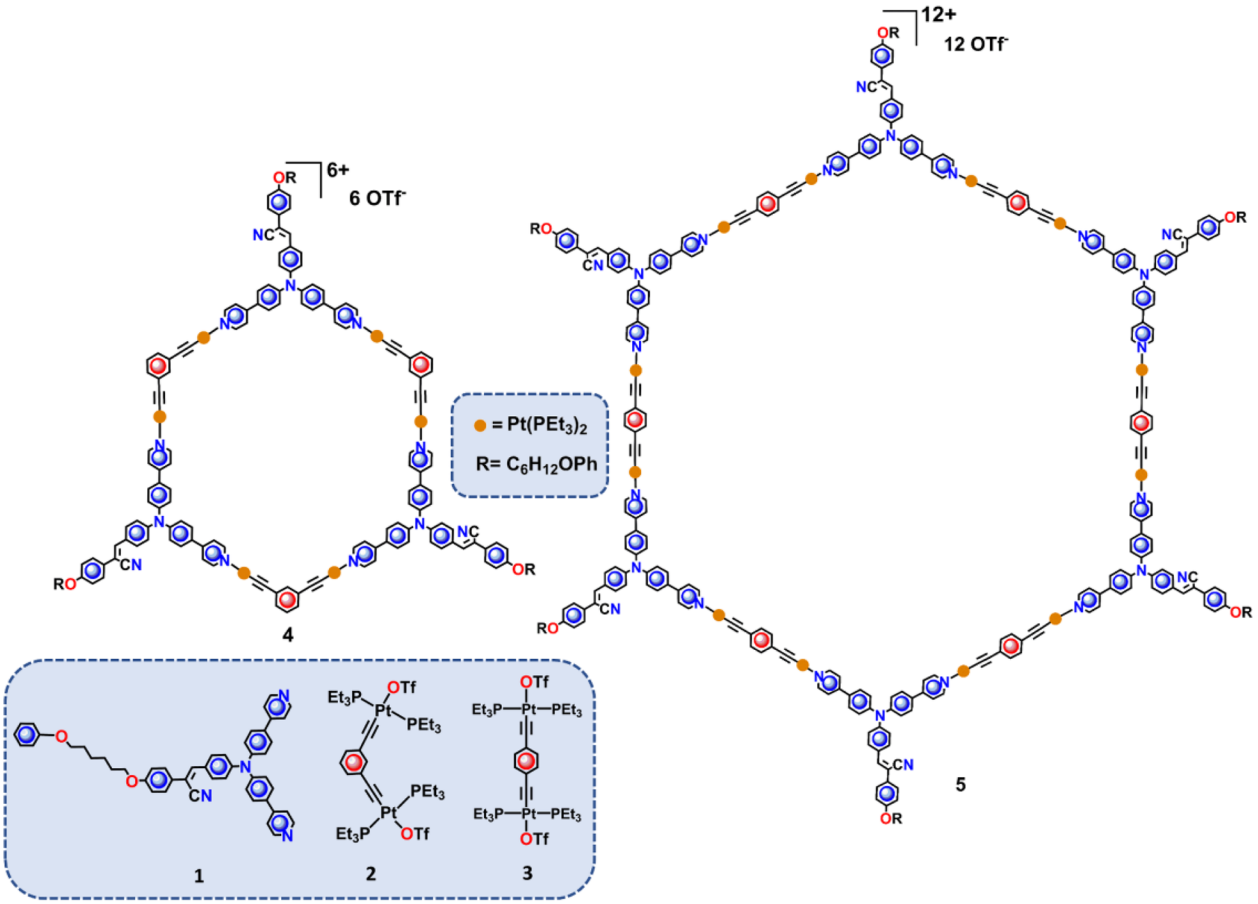

Figure 1. Metallacycles **4** and **5** and the building blocks **1**, **2**, and **3**.

form supramolecular assemblies, and in their closely packed state they will not suffer fluorescence quenching and, thus, could serve as an excellent platform for light harvesting.

The hexagonal [3+3] metallacycle **4** was readily accessible by stirring an equal molar mixture of **1** and Pt-acceptor **2** in a mixed solvent system of dichloromethane–methanol (1:1; v/v) at room temperature for 6 h; a [6+6] metallacycle **5** was obtained from **1** and Pt-acceptor **3** under similar reaction conditions (Schemes S2 and S3). The metallacycles were obtained as yellow solids upon addition of diethyl ether onto the reaction mixtures and were characterized by various spectroscopic techniques, including ^{1}H NMR, ^{31}P{^{1}H} NMR, ^{1}H–^{1}H COSY, and 2D diffusion-ordered ^{1}H NMR spectroscopy (DOSY) and electrospray ionization time-of-flight mass spectrometry (ESI-TOF-MS) analysis (Figures S1–S14).

In the ^{1}H NMR spectrum of **4**, characteristic NMR signals corresponding to **1** and the Pt-acceptor **2** observed at around 8.57 and 7.12–7.19 ppm, respectively, with a 1:1 intensity ratio, indicated the formation of a [3+3] assembly (Figures 2a and S4). Similarly, metallacycle **5** formation was indicated by ^{1}H NMR signals with a 1:1 intensity ratio, corresponding to the ligand **1** and Pt-acceptor **3** at around 8.56 and 7.19 ppm, respectively (Figure S8). The ^{31}P{^{1}H} NMR spectra of both metallacycles displayed sharp singlet peaks (Figures 2b and S9) with concomitant ^{195}Pt satellites (δ = 16.06 and 16.30 ppm for **4** and **5**, respectively), which indicated the presence of only one type of phosphorus in the assemblies, confirming the formation of highly symmetric structures. An upfield shift of ~6 ppm was observed in the ^{31}P{^{1}H} NMR of the metallacycles with respect to their corresponding Pt-building blocks, attributed to the metal–ligand coordination. The stoichiometry of the formation of metallacycles **4** and **5** was confirmed by ESI-TOF-MS analysis. For metallacycle **4**, isotopic patterns of the peaks at m/z 1053.24 and 852.84 Da for the $[M - 5OTf]^{5+}$ and $[M - 6OTf]^{6+}$, respectively, match well with their calculated isotopic distribution patterns (Figure 2c). In contrast, the larger metallacycle **5** shows a peak at m/z 1186.82 Da for $[M - 9OTf]^{9+}$; however, the isotopic distribution pattern suggests that the peak is actually due to two fragments, X^{3+} and Y^{6+}(Figures S11 and S12), resulting from $[M - 9OTf]^{9+}$.

Moreover, single diffusion bands at 7.6×10^{-9} and 3.6×10^{-9} m^2/s in the ^{1}H DOSY NMR spectra (Figures S13 and S14) of **4** and **5**, respectively, are in agreement with the formation of a single product in the reaction. To gain further insight into the structural characteristics of the metallacycles, PM6 semiempirical calculations were carried out, where the ethyl groups of the phosphine ligands were modeled as hydrogen atoms. The computational results indicate that the metallacycles have an almost planar hexagonal backbone, with internal cavity sizes of around 3.2 and 6.6 nm for **4** and **5**, respectively (Figures S15 and S16).

The photophysical properties of the metallacycles were investigated in DMSO. The UV–vis spectrum of **4** exhibits two absorption bands at around 300 and 400 nm, whereas **5** has absorption bands at around 340 and 400 nm (Figures S17 and S18). Upon excitation at 410 nm, both metallacycles display similar emission patterns with an emission maximum at

DOI: 10.1021/jacs.9b08403
J. Am. Chem. Soc. 2019, 141, 14565–14569

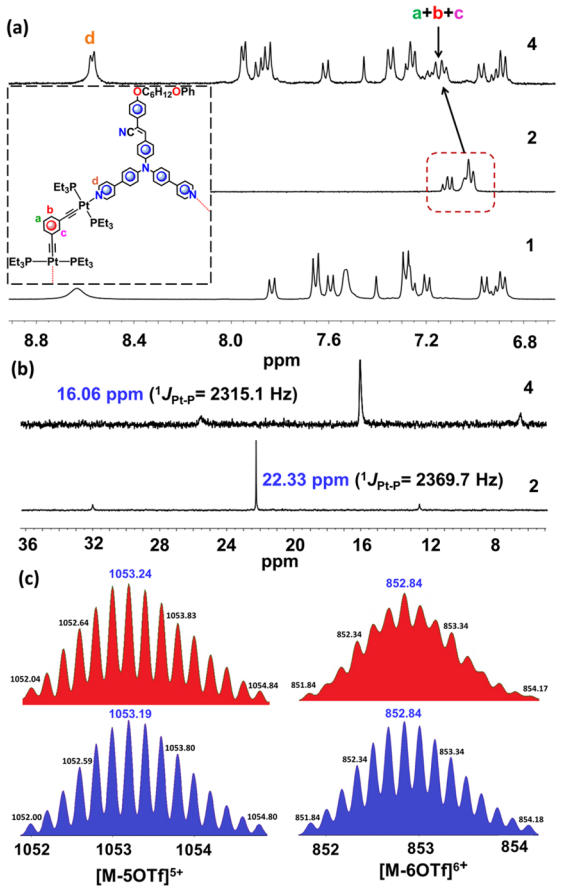

Figure 2. (a) ^{1}H NMR (400 MHz, CD_2Cl_2, 298 K) and (b) $^{31}P\{^1H\}$ NMR (121.4 MHz, CD_2Cl_2, 298 K) spectra of the metallacycle **4** and its building blocks. (c) Experimental (red) and calculated (blue) ESI-TOF-MS spectra of **4**.

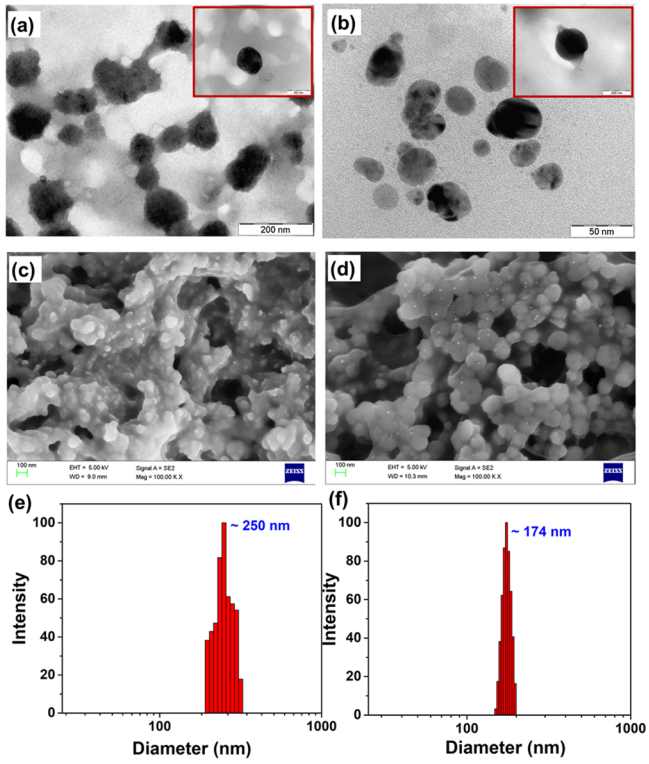

Figure 3. TEM images of (a) **4** and (b) **5**, SEM images of (c) **4** and (d) **5**, and DLS profiles of (e) **4** and (f) **5** in H_2O–DMSO (4:1; v/v). Insets: TEM image of a single spherical particle.

521 nm (Figure S19). The absorption and emission of the metallacycles were also investigated in various solvents, which did not indicate any significant solvatochromic characteristics (Figure S20). With increasing water content in the DMSO solution of the metallacycle (**4** or **5**), a substantial increase in fluorescence intensity is observed (Figures S21 and S22), as expected due to the presence of the cyanostilbene moieties that facilitate AIEE. The highest emission intensity was observed in 80% H_2O–DMSO, while further a increase in water fraction leads to a decrease in emission intensity, presumably due to precipitation of the metallacycles. This AIEE behavior is also supported by a sharp increase in the fluorescence quantum yields (φ) of the metallacycles in the solid state and in the aggregates (**4**^{a} and **5**^{a}). For instance, the fluorescence quantum yield of **4** was found to be 28% in the solid state and 17% in a H_2O–DMSO (4:1; v/v) solvent system, which are substantially higher than the quantum yield of the metallacycle in the DMSO solution (φ = 9%). A similar trend was observed with metallacycle **5**, which has fluorescence quantum yields of 33%, 28%, and 10% in the solid state, in a H_2O–DMSO solvent system (4:1; v/v), and in a DMSO solution, respectively (Table S1).[18]

The morphologies of the metallacycles in the aggregated state were investigated by scanning electronic microscopy (SEM) and transmission electron microscopy (TEM). The TEM analysis (Figure 3a,b) shows the formation of spherical particles, while the SEM analysis suggests an agglomeration of these spherical particles (Figure 3c,d). Dynamic light scattering (DLS) experiments (Figure 3e,f) provided average hydrodynamic diameters of the aggregates of around 250 and 174 nm for **4** and **5**, respectively, in H_2O–DMSO (4:1; v/v).

These results indicated that a H_2O–DMSO (4:1; v/v) solvent system would be the best medium to investigate the light-harvesting property of the metallacycles, as under such aggregated state the metallacycles showed the highest fluorescence emission without any self-quenching and precipitation from the solution. To prepare the LHSs, we used the fluorescent dye Eosin Y (ESY) as a fluorescence energy acceptor. It is worth noting that, for efficient energy transfer, the absorption band of the acceptor should overlap with the emission band of the donor. The UV–vis spectrum of ESY in H_2O–DMSO has an absorption band from 430 to 550 nm with an absorption maximum at 520 nm. As shown in Figure S23, the absorption spectrum of ESY and the emission spectra of the metallacycles overlap well, suggesting the possibility of energy transfer from the metallacycles to ESY. When a 1 μM solution (H_2O–DMSO, 4:1, v/v) of ESY was gradually added to a 3 mL, 1 μM solution (H_2O–DMSO, 4:1, v/v) of a metallacycle (**4** or **5**), a sharp decrease in emission intensity of the metallacycle was observed (Figure 4a,b), and the fluorescence intensity corresponding to ESY was found to increase upon excitation at 410 nm. In contrast, under similar conditions, ESY alone was found to be non-emissive upon excitation at 410 nm (Figure S24), ruling out the possibility of direct excitation of ESY. Moreover, a substantial increase in the quantum yields of the metallacycles was observed in the presence of ESY, which suggests that ESY accepts and emits most of the excitation energy. The energy transfer efficiencies are calculated as 65% and 52% in the **4**^{a}**+ESY** and **5**^{a}**+ESY**

DOI: 10.1021/jacs.9b08403
J. Am. Chem. Soc. 2019, 141, 14565–14569

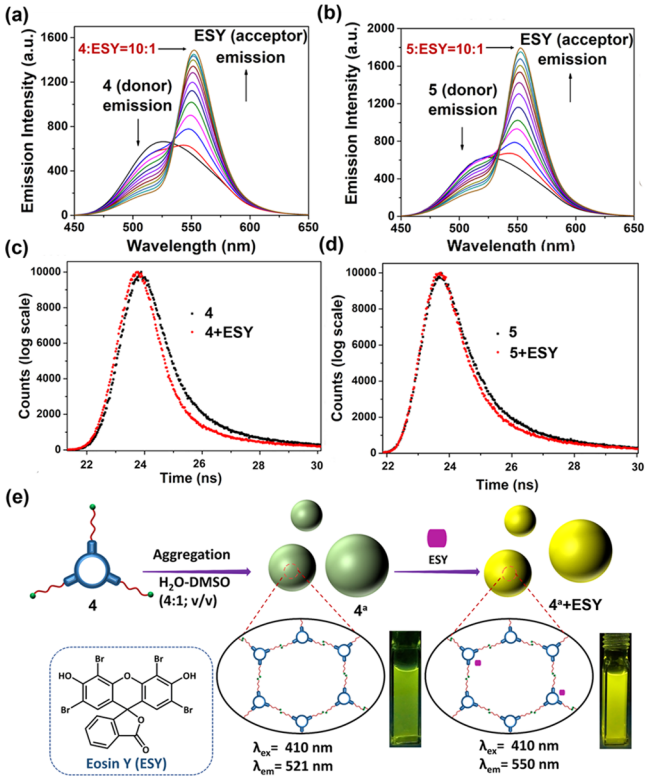

Figure 4. Fluorescence spectra of the metallacycles (a) **4** and (b) **5** with gradual addition of ESY (λ_{ex} = 410 nm) in H_2O−DMSO (4:1; v/v). Change in the fluorescence decay profiles of the metallacycles (c) **4** and (d) **5** in the presence of ESY (metallacycle:ESY = 20:1) in H_2O−DMSO (4:1; v/v). (e) Cartoon representation of light-harvesting system generated from **4** and ESY, with visible color change of the solution under 365 nm UV light in H_2O−DMSO (4:1; v/v).

systems, respectively, at a 10:1 donor/acceptor ratio, which are comparable with the efficiencies of some of the recently reported single-molecule-based supramolecular light-harvesting systems.[15,19]

The best way to understand the energy transfer process is to measure the fluorescence lifetime of the donor in the presence of the acceptor. Therefore, fluorescence decay experiments were carried out to support the occurrence of the light-harvesting process. The fluorescence lifetime of the metallacycle **4** (τ_1 = 0.75 ns and τ_2 = 2.94 ns) was found to be higher than the fluorescence lifetime of **4** in the presence of ESY (τ_1 = 0.51 ns and τ_2 = 2.65 ns) (Figure 4c). Similarly, the fluorescence lifetime of the assembly of **5** and ESY (τ_1= 0.57 ns and τ_2 = 2.86 ns) was found to be shorter (Figure 4d) than the fluorescence lifetime of **5** (τ_1 = 0.75 ns and τ_2 = 2.97 ns). These results indicate that the energy transfer takes place from the metallacycle to the ESY (Figure 4e).

In conclusion, two fluorescent hexagonal metallacycles (**4** and **5**) were devised to construct artificial light-harvesting systems. The metallacycles were found to have good fluorescence properties and AIEE characteristics. Most importantly, simple mixing of the acceptor (Eosin Y) and a metallacycle results in an efficient Förster resonance energy transfer (FRET) process between the metallacycle and ESY, leading to the in situ formation of an efficient artificial LHS. These artificial LHSs exhibit good energy transfer efficiencies, as high as 65% in the **4**^{a}**+ESY** system at a 10:1 donor/acceptor ratio. We anticipate that understanding the light-harvesting properties in such supramolecular coordination complexes will open up new possibilities for the design and fabrication of LHSs in the future.

■ ASSOCIATED CONTENT

Supporting Information

The Supporting Information is available free of charge on the ACS Publications website at DOI: 10.1021/jacs.9b08403.

Experimental details and characterization data of all new compounds, including Schemes S1−S3, Figures S1−S26, and Tables S1 and S2 (PDF)

■ AUTHOR INFORMATION

Corresponding Authors

*koushikchemistry@gmail.com
*psm@iisc.ac.in
*stang@chem.utah.edu

ORCID

Koushik Acharyya: 0000-0003-0213-2712
Soumalya Bhattacharyya: 0000-0003-4467-6056
Hajar Sepehrpour: 0000-0003-1638-2755
Shubhadip Chakraborty: 0000-0002-2982-6450
Xiaopeng Li: 0000-0001-9655-9551
Partha Sarathi Mukherjee: 0000-0001-6891-6697
Peter J. Stang: 0000-0002-2307-0576

Notes

The authors declare no competing financial interest.

■ ACKNOWLEDGMENTS

P.J.S. thanks the U.S. National Institutes of Health (Grant R01 CA215157) for financial support. P.S.M. thanks the SERB (India) for financial support (Grant No. CRG/2018/000315). S.B. thanks CSIR India for research fellowship. K.A. is thankful to Heng Wang and Ruidong Ni for their help in ESI-TOF-MS analysis.

■ REFERENCES

(1) McDermott, G.; Prince, S. M.; Freer, A. A.; Hawthornthwaite-Lawless, A. M.; Papiz, M. Z.; Cogdell, R. J.; Isaacs, N. W. Crystal structure of an integral membrane light-harvesting complex from photosynthetic bacteria. *Nature* **1995**, *374*, 517−521.

(2) (a) Ziessel, R.; Ulrich, G.; Haefele, A.; Harriman, A. An Artificial Light-Harvesting Array Constructed from Multiple Bodipy Dyes. *J. Am. Chem. Soc.* **2013**, *135*, 11330−11344. (b) Shi, Y.; Cao, X.; Hu, D.; Gao, H. Highly Branched Polymers with Layered Structures that Mimic Light-Harvesting Processes. *Angew. Chem., Int. Ed.* **2018**, *57*, 516−520.

(3) (a) Ajayaghosh, A.; Praveen, V. K.; Vijayakumar, C.; George, S. J. Molecular Wire Encapsulated into π Organogels: Efficient Supramolecular Light-Harvesting Antennae with Color-Tunable Emission. *Angew. Chem., Int. Ed.* **2007**, *46*, 6260−6265. (b) Ardoña, H. A. M.; Draper, E. R.; Citossi, F.; Wallace, M.; Serpell, L. C.; Adams, D. J.; Tovar, J. D. Kinetically Controlled Coassembly of Multichromophoric Peptide Hydrogelators and the Impacts on Energy Transport. *J. Am. Chem. Soc.* **2017**, *139*, 8685−8692.

(4) (a) Calver, C. F.; Schanze, K. S.; Cosa, G. Biomimetic Light-Harvesting Antenna Based on the Self-Assembly of Conjugated Polyelectrolytes Embedded within Lipid Membranes. *ACS Nano* **2016**, *10*, 10598−10605. (b) Okazawa, Y.; Kondo, K.; Akita, M.; Yoshizawa, M. Polyaromatic Nanocapsules Displaying Aggregation-Induced Enhanced Emissions in Water. *J. Am. Chem. Soc.* **2015**, *137*, 98−101.

DOI: 10.1021/jacs.9b08403
J. Am. Chem. Soc. 2019, 141, 14565−14569

(5) (a) Liu, Y.; Jin, J.; Deng, H.; Li, K.; Zheng, Y.; Yu, C.; Zhou, Y. Protein-Framed Multi-Porphyrin Micelles for a Hybrid Natural–Artificial Light-Harvesting Nanosystem. *Angew. Chem., Int. Ed.* **2016**, *55*, 7952–7957. (b) Li, C.; Zhang, J.; Zhang, S.; Zhao, Y. Efficient Light-Harvesting Systems with Tunable Emission through Controlled Precipitation in Confined Nanospace. *Angew. Chem., Int. Ed.* **2019**, *58*, 1643–1647.

(6) (a) Li, J.-J.; Chen, Y.; Yu, J.; Cheng, N.; Liu, Y. A Supramolecular Artificial Light-Harvesting System with an Ultrahigh Antenna Effect. *Adv. Mater.* **2017**, *29*, 1701905. (b) Guo, S.; Song, Y.; He, Y.; Hu, X.-Y.; Wang, L. Highly Efficient Artificial Light-Harvesting Systems Constructed in Aqueous Solution Based on Supramolecular Self-Assembly. *Angew. Chem., Int. Ed.* **2018**, *57*, 3163–3167.

(7) (a) Williams, D. E.; Rietman, J. A.; Maier, J. M.; Tan, R.; Greytak, A. B.; Smith, M. D.; Krause, J. A.; Shustova, N. B. Energy Transfer on Demand: Photoswitch-Directed Behavior of Metal–Porphyrin Frameworks. *J. Am. Chem. Soc.* **2014**, *136*, 11886–11889. (b) Lee, H.; Jeong, Y.-H.; Kim, J.-H.; Kim, I.; Lee, E.; Jang, W.-D. Supramolecular Coordination Polymer Formed from Artificial Light-Harvesting Dendrimer. *J. Am. Chem. Soc.* **2015**, *137*, 12394–12399.

(8) (a) Winiger, C. B.; Li, S.; Kumar, G. R.; Langenegger, S. M.; Häner, R. Long-Distance Electronic Energy Transfer in Light-Harvesting Supramolecular Polymers. *Angew. Chem., Int. Ed.* **2014**, *53*, 13609–13613. (b) Jiang, Y.; McNeill, J. Light-Harvesting and Amplified Energy Transfer in Conjugated Polymer Nanoparticles. *Chem. Rev.* **2017**, *117*, 838–859.

(9) (a) Sato, S.; Iida, J.; Suzuki, K.; Kawano, M.; Ozeki, T.; Fujita, M. Fluorous Nanodroplets Structurally Confined in an Organo-palladium Sphere. *Science* **2006**, *313*, 1273–1276. (b) Pluth, M. D.; Bergman, R. G.; Raymond, K. N. Acid Catalysis in Basic Solution: A Supramolecular Host Promotes Orthoformate Hydrolysis. *Science* **2007**, *316*, 85–88. (c) Park, K.-M.; Kim, S.-Y.; Heo, J.; Whang, D.; Sakamoto, S.; Yamaguchi, K.; Kim, K. Designed Self-Assembly of Molecular Necklaces. *J. Am. Chem. Soc.* **2002**, *124*, 2140–2147. (d) Freye, S.; Michel, R.; Stalke, D.; Pawliczek, M.; Frauendorf, H.; Clever, G. H. Template Control over Dimerization and Guest Selectivity of Interpenetrated Coordination Cages. *J. Am. Chem. Soc.* **2013**, *135*, 8476–8479. (e) Li, S.; Huang, J.; Cook, T. R.; Pollock, J. B.; Kim, H.; Chi, K.-W.; Stang, P. J. Formation of [3]Catenanes from 10 Precursors via Multicomponent Coordination-Driven Self-Assembly of Metallarectangles. *J. Am. Chem. Soc.* **2013**, *135*, 2084–2087. (f) Chakrabarty, R.; Mukherjee, P. S.; Stang, P. J. Supramolecular Coordination: Self-Assembly of Finite Two- and Three-Dimensional Ensembles. *Chem. Rev.* **2011**, *111*, 6810–6918. (g) Forgan, R. S.; Sauvage, J.-P.; Stoddart, J. F. Chemical Topology: Complex Molecular Knots, Links, and Entanglements. *Chem. Rev.* **2011**, *111*, 5434–5464. (h) Ayme, J.-F.; Beves, J. E.; Leigh, D. A.; McBurney, R. T.; Rissanen, K.; Schultz, D. Pentameric Circular Iron(II) Double Helicates and a Molecular Pentafoil Knot. *J. Am. Chem. Soc.* **2012**, *134*, 9488–9497. (i) Saha, M. L.; Schmittel, M. From 3-Fold Completive Self-Sorting of a Nine-Component Library to a Seven-Component Scalene Quadrilateral. *J. Am. Chem. Soc.* **2013**, *135*, 17743–17746. (j) Yan, X.; Jiang, B.; Cook, T. R.; Zhang, Y.; Li, J.; Yu, Y.; Huang, F.; Yang, H.-B.; Stang, P. J. Dendronized Organoplatinum(II) Metallacyclic Polymers Constructed by Hierarchical Coordination-Driven Self-Assembly and Hydrogen-Bonding Interfaces. *J. Am. Chem. Soc.* **2013**, *135*, 16813–16816. (k) Sun, Y.; Li, S.; Zhou, Z.; Saha, M. L.; Datta, S.; Zhang, M.; Yan, X.; Tian, D.; Wang, H.; Wang, L.; Li, X.; Liu, M.; Li, H.; Stang, P. J. Alanine-Based Chiral Metallogels via Supramolecular Coordination Complex Platforms: Metallogelation Induced Chirality Transfer. *J. Am. Chem. Soc.* **2018**, *140*, 3257–3263.

(10) (a) Brown, C. J.; Toste, F. D.; Bergman, R. G.; Raymond, K. N. Supramolecular Catalysis in Metal–Ligand Cluster Hosts. *Chem. Rev.* **2015**, *115*, 3012–3035. (b) Yoshizawa, M.; Tamura, M.; Fujita, M. Diels-Alder in Aqueous Molecular Hosts: Unusual Regioselectivity and Efficient Catalysis. *Science* **2006**, *312*, 251–254.

(11) (a) Tang, J.-H.; Sun, Y.; Gong, Z.-L.; Li, Z.-Y.; Zhou, Z.; Wang, H.; Li, X.; Saha, M. L.; Zhong, Y.-W.; Stang, P. J. Temperature-Responsive Fluorescent Organoplatinum(II) Metallacycles. *J. Am. Chem. Soc.* **2018**, *140*, 7723–7729. (b) Chen, L.-J.; Ren, Y.-Y.; Wu, N.-W.; Sun, B.; Ma, J.-Q.; Zhang, L.; Tan, H.; Liu, M.; Li, X.; Yang, H.-B. Hierarchical Self-Assembly of Discrete Organoplatinum(II) Metallacycles with Polysaccharide via Electrostatic Interactions and Their Application for Heparin Detection. *J. Am. Chem. Soc.* **2015**, *137*, 11725–11735.

(12) (a) Vajpayee, V.; Yang, Y. J.; Kang, S. C.; Kim, H.; Kim, I. S.; Wang, M.; Stang, P. J.; Chi, K.-W. Hexanuclear self-assembled arene-ruthenium nano-prismatic cages: potential anticancer agents. *Chem. Commun.* **2011**, *47*, 5184–5186. (b) Mattsson, J.; Zava, O.; Renfrew, A. K.; Sei, Y.; Yamaguchi, K.; Dyson, P. J.; Therrien, B. Drug delivery of lipophilic pyrenyl derivatives by encapsulation in a water soluble metalla-cage. *Dalton Trans* **2010**, *39*, 8248–8255. (c) Fujita, D.; Suzuki, K.; Sato, S.; Yagi-Utsumi, M.; Yamaguchi, Y.; Mizuno, N.; Kumasaka, T.; Takata, M.; Noda, M.; Uchiyama, S.; Kato, K.; Fujita, M. Protein encapsulation within synthetic molecular hosts. *Nat. Commun.* **2012**, *3*, 1093. (d) Sepehrpour, H.; Fu, W.; Sun, Y.; Stang, P. J. Biomedically Relevant Self-Assembled Metallacycles and Metallacages. *J. Am. Chem. Soc.* **2019**, DOI: 10.1021/jacs.9b06222.

(13) Samanta, D.; Mukherjee, P. S. Structural Diversity in Multinuclear PdII Assemblies that Show Low-Humidity Proton Conduction. *Chem. - Eur. J.* **2014**, *20*, 5649–5656.

(14) (a) Zhang, C.-W.; Ou, B.; Jiang, S.-T.; Yin, G.-Q.; Chen, L.-J.; Xu, L.; Li, X.; Yang, H.-B. Cross-linked AIE supramolecular polymer gels with multiple stimuli-responsive behaviours constructed by hierarchical self-assembly. *Polym. Chem.* **2018**, *9*, 2021–2030. (b) Yan, X.; Cook, T. R.; Wang, P.; Huang, F.; Stang, P. J. Highly emissive platinum(II) metallacages. *Nat. Chem.* **2015**, *7*, 342. (c) Zhou, Z.; Chen, D.-G.; Saha, M. L.; Wang, H.; Li, X.; Chou, P.-T.; Stang, P. J. Designed Conformation and Fluorescence Properties of Self-Assembled Phenazine-Cored Platinum(II) Metallacycles. *J. Am. Chem. Soc.* **2019**, *141*, 5535–5543. (d) Bhattacharyya, S.; Chowdhury, A.; Saha, R.; Mukherjee, P. S. Multifunctional Self-Assembled Macrocycles with Enhanced Emission and Reversible Photochromic Behavior. *Inorg. Chem.* **2019**, *58*, 3968–3981.

(15) Zhang, Z.; Zhao, Z.; Hou, Y.; Wang, H.; Li, X.; He, G.; Zhang, M. Aqueous Platinum(II)-Cage-Based Light-Harvesting System for Photocatalytic Cross-Coupling Hydrogen Evolution Reaction. *Angew. Chem., Int. Ed.* **2019**, *58*, 8862–8866.

(16) (a) Shi, B.; Liu, Y.; Zhu, H.; Vanderlinden, R. T.; Shangguan, L.; Ni, R.; Acharyya, K.; Tang, J.-H.; Zhou, Z.; Li, X.; Huang, F.; Stang, P. J. Spontaneous Formation of a Cross-Linked Supramolecular Polymer Both in the Solid State and in Solution, Driven by Platinum(II) Metallacycle-Based Host–Guest Interactions. *J. Am. Chem. Soc.* **2019**, *141*, 6494–6498. (b) Shi, B.; Zhou, Z.; Vanderlinden, R. T.; Tang, J.-H.; Yu, G.; Acharyya, K.; Sepehrpour, H.; Stang, P. J. Spontaneous Supramolecular Polymerization Driven by Discrete Platinum Metallacycle-Based Host–Guest Complexation. *J. Am. Chem. Soc.* **2019**, *141*, 11837–11841.

(17) An, B.-K.; Gierschner, J.; Park, S. Y. π-Conjugated Cyanostilbene Derivatives: A Unique Self-Assembly Motif for Molecular Nanostructures with Enhanced Emission and Transport. *Acc. Chem. Res.* **2012**, *45*, 544–554.

(18) The ligand **1** has absolute fluorescent quantum yields of 7%, 11%, and 17% in DMSO, in H_2O–DMSO (4:1; v/v), and in the solid state, respectively.

(19) Li, Y.; Dong, Y.; Cheng, L.; Qin, C.; Nian, H.; Zhang, H.; Yu, Y.; Cao, L. Aggregation-Induced Emission and Light-Harvesting Function of Tetraphenylethene-Based Tetracationic Dicyclophane. *J. Am. Chem. Soc.* **2019**, *141*, 8412–8415.

DOI: 10.1021/jacs.9b08403
J. Am. Chem. Soc. 2019, 141, 14565–14569